VIP Ethylene Detection

DOI: 10.1002/anie.201201042

Selective Detection of Ethylene Gas Using Carbon Nanotube-based Devices: Utility in Determination of Fruit Ripeness**

*Birgit Esser, Jan M. Schnorr, and Timothy M. Swager**

Ethylene, the smallest plant hormone, plays a role in many developmental processes in plants. For example, it initiates the ripening of fruit, promotes seed germination and flowering, and is responsible for the senescence of leaves and flowers.[1] The rate-limiting step in the biosynthetic pathway to ethylene, elucidated by Yang et al., is catalyzed by 1-aminocyclopropane-1-carboxylic acid (ACC) synthase.[2] Ethylene production in plants is induced during several developmental stages as well as by external factors. The ripening process is the result of ethylene binding to the receptor ETR1, which leads to the translation of ripening genes and eventually the production of enzymes that induce the visible effects of ripening. The monitoring of the ethylene concentration is of utmost importance in the horticultural industries. The internal ethylene concentration in fruit can serve as an indicator for determining the time of harvest, while the monitoring of the atmospheric ethylene level in storage facilities and during transportation is crucial for avoiding overripening of fruit.

We herein present a reversible chemoresistive sensor that is able to detect sub-ppm concentrations of ethylene. Our detection method has high selectivity towards ethylene and is simply prepared in few steps from commercially available materials. The sensing mechanism relies on the high sensitivity in resistance of single-walled carbon nanotubes (SWNTs) to changes in their electronic surroundings. These principles have been employed in a variety of sensing applications.[3] For the selective recognition of ethylene we employ a copper(I) complex, inspired by nature, where Cu^{I} has been found to be an essential cofactor of the receptor ETR1.[4] As a result of its small size and lack of polar chemical functionality, ethylene is generally hard to detect. Traditionally, ethylene concentrations are monitored through gas chromatography[5a] or laser acoustic spectroscopy,[5b] which both require expensive instrumentation and are not suitable for in-field measurements. Other techniques suggested are based on amperometric[5c] or electrochemical[5d] methods or rely on changes in luminescence properties.[5e,6] Furthermore, gas-sampling tubes based on a colorimetric reaction are available.[1] The carbon nanotube based sensing concept we have developed is shown in Scheme 1.

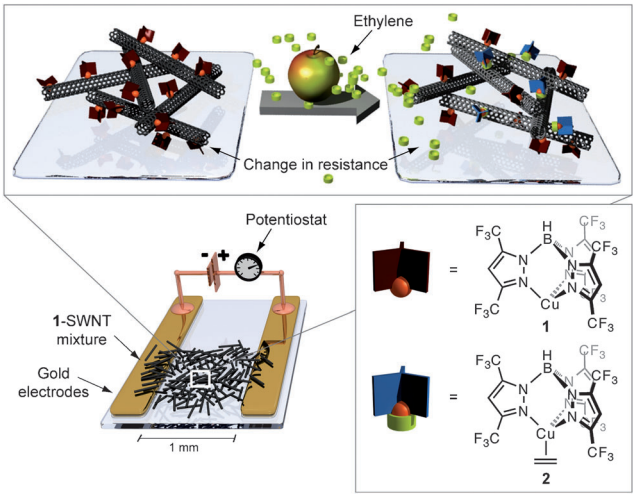

Scheme 1. Ethylene detection by a chemoresistive sensor: A mixture of single-walled carbon nanotubes (SWNTs) and copper complex **1** is drop-cast between gold electrodes, and the change in resistance in response to ethylene exposure is measured. The copper complexes partly bind to ethylene molecules, resulting in a resistance change.

The ethylene-sensitive material is an intimate mixture of SWNTs with a copper(I) complex **1** based upon a fluorinated tris(pyrazolyl)borate ligand, which is able to interact with the surface of carbon nanotubes, thereby influencing their conductivity. Upon exposure to ethylene, **1** binds to ethylene and forms complex **2**, which has a decreased interaction with the SWNT surface. The result of this transformation is an increase in resistance of the SWNT network. Our choice of the copper–ligand system **1** is based on the fact that **2** is one of the most stable copper–ethylene complexes known.[7] It is not easily oxidized under ambient conditions and is stable in high vacuum. Compound **1** has been employed in the detection of ethylene in fluorescence-based sensors.[6]

In a typical experiment, **1** is ultrasonicated with SWNTs in a mixture of *o*-dichlorobenzene and toluene (2:3). Devices are prepared by drop-casting the resulting dispersion onto glass slides with pre-deposited gold electrodes (as shown in Scheme 1). The experimental setup for sensing measurements is shown in Scheme 2. The device is enclosed in a gas flow chamber, with its electrodes connected to a potentiostat. The analyte–gas mixture is produced in a gas generator in which

[*] Dr. B. Esser, J. M. Schnorr, Prof. Dr. T. M. Swager
Department of Chemistry and Institute for Soldier Nanotechnologies, Massachusetts Institute of Technology
Cambridge, MA 02139 (USA)
E-mail: tswager@mit.edu

[**] This research was supported (in part) by the U.S. Army Research Office under contract W911NF-07-D-0004. B.E. is grateful to the German Academy of Sciences Leopoldina for a postdoctoral fellowship (LPDS 2009-8). We thank S. L. Buchwald for the usage of computational resources, J. J. Walish for fabricating the device holder, and J. G. Weis for SEM measurements.

Supporting information for this article is available on the WWW under http://dx.doi.org/10.1002/anie.201201042.

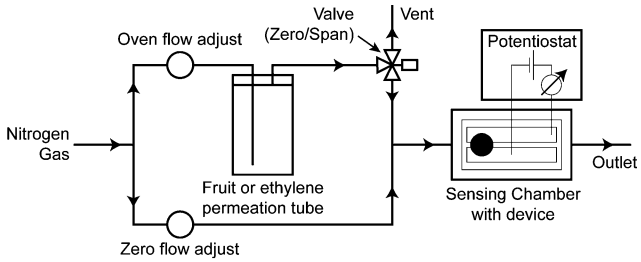

Scheme 2. Experimental setup for sensing measurements: A continuous gas flow is directed through the device chamber. The gas stream can be switched between nitrogen gas ("zero" mode) or the nitrogen gas analyte mixture ("span" mode), in which the gas stream runs through the flow chamber containing the analyte (ethylene) or a piece of fruit.

a stream of nitrogen gas is split into two parts, one of which is led through a flow chamber containing an ethylene permeation tube or a piece of fruit. During a measurement, a continuous gas stream of constant flow rate, which can be switched between dinitrogen and the analyte–dinitrogen mixture, is directed over the device. The results from exposing **1**-SWNT devices to low concentrations of ethylene are shown in Figure 1. We were able to detect ethylene concentrations of less than 1 ppm and performed measurements up to 50 ppm. 1 ppm is the concentration at which ripening occurs at the maximum rate for many commodities.[1] Within the range of concentrations measured (0.5–50 ppm), we observe a linear change in response (see Figure 1 c).

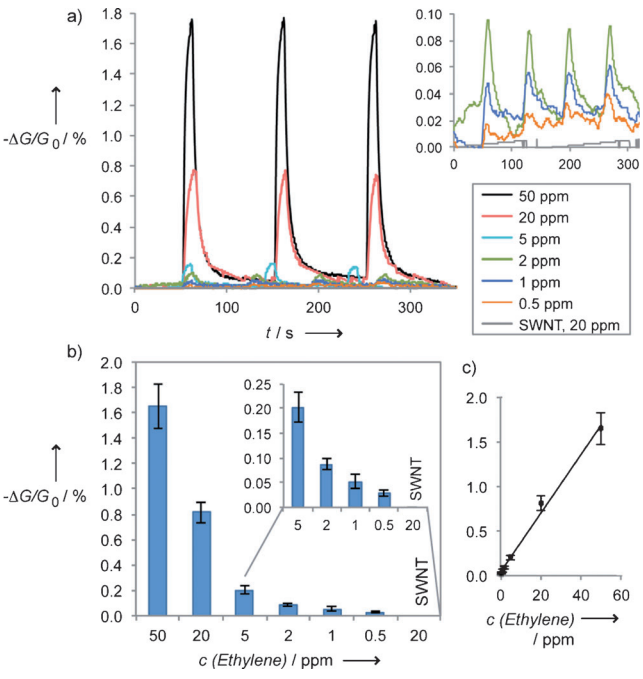

Figure 1. a) Relative responses of **1**-SWNT devices to 0.5, 1, 2, 5, 20, and 50 ppm ethylene diluted with nitrogen gas and of pristine SWNT to 20 ppm ethylene (inset:[8] responses of **1**-SWNT to 0.5, 1, and 2 ppm and of SWNT to 20 ppm); b) average responses from three different devices each and c) plot of average response vs. ethylene concentration.

Devices made from pristine SWNTs show no response to the same concentrations of ethylene (Figure 1). Further controls, in which $[Cu(CH_3CN)_4]PF_6$ or the sodium equivalent of **1** (Cu replaced by Na) were employed instead of **1**, did not respond to ethylene either (see the Supporting Information). Employing the ethylene complex **2** resulted in device sensitivity towards 20 ppm ethylene; however, the response amounts to only about 25% of that of **1**-SWNT devices (see the Supporting Information). In optimizing the ratio of **1** to SWNT, we found that a large excess of **1** (ratio of **1** to SWNT carbon atoms 1:6) resulted in the best sensitivity. We tested different types of commercially available SWNTs in our devices (see the Supporting Information). The best results were obtained with SWNTs of small diameter, namely SWNTs containing more than 50% of (6,5) chirality. We assume that the stronger curvature of the carbon nanotube surface enhances the interaction between **1** and the SWNT.

Upon exposure to ethylene, a reversible increase in resistance is observed. We ascribe this to a mechanism as shown in Scheme 1, where the interaction of **1** with the SWNT surface induces doping of the nanotubes. When complexes **1** bind to ethylene, this doping effect is diminished, and hence an increase in resistance is measured. To rationalize the interaction between **1** and the SWNT surface, we performed model calculations using density functional theory. We optimized the structure of complex **3**, where the copper center in **1** is bound to the surface of a short segment of a (6,5) SWNT using the B3LYP functional with the 6-31G* basis set for main-group elements and LanL2DZ for Cu.[9] The optimized structure of **3** is shown in Figure 2. Steric interactions force one of the pyrazol rings of the ligand to be twisted in such a way that a trigonal-planar coordination results for the Cu center. In an isodesmic equation, the binding strength of **1** to a (6,5) SWNT fragment (**3**) was compared to the binding in **2**. The calculation suggests that **2** is strongly favored over **3** (by 70–80 kcal mol^{-1}).[10] Since we observe reversible responses to ethylene, we assume that the copper complexes **1** do not completely dissociate from the SWNTs but bind the ethylene molecules in an associative fashion.

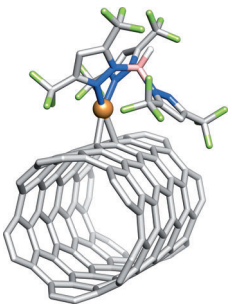

Figure 2. Optimized structure of **3** in which **1** is coordinatively bound to a (6,5) SWNT fragment (B3LYP/6-31G*, LanL2DZ for Cu; hydrogen atoms at the ends of the SWNT fragment and on the pyrazol rings have been omitted for clarity).

The Raman and IR spectra of **1**-SWNT are shown in Figure 3. Upon introduction of **1** into the SWNT network, a slight shift of the G and G' bands in the Raman spectrum to lower energies is observed, which can be indicative of p-type doping.[11] The IR spectrum of **1**-SWNT is dominated by the C–F stretching modes of the ligand between 1080–1260 cm^{-1}. The ν_{BH} shift is found at 2607 cm^{-1}. X-ray photoelectron spectroscopy (XPS) measurements were used to confirm the ratio of **1** to SWNTs and to investigate the oxidation state of the copper centers, which can undergo oxidation to copper(II). We found a ratio of 1:22 for C_{SWNT}/Cu (based on the

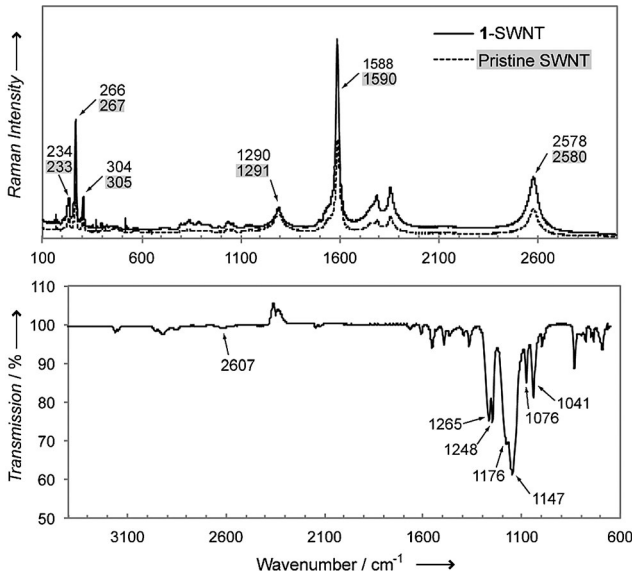

Figure 3. Top: Raman spectra of **1**-SWNT and pristine SWNT (dashed line; laser energy 785 nm); bottom: IR spectrum of **1**-SWNT.

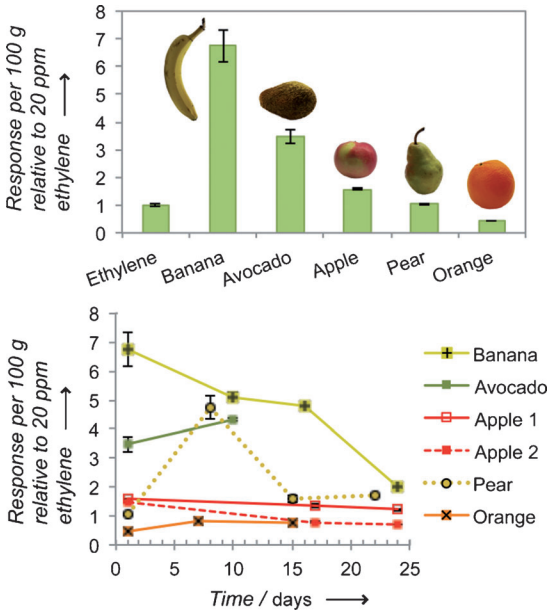

Figure 4. Top: Responses of **1**-SWNT devices to 100 g of different fruit relative to 20 ppm ethylene; bottom: responses to fruit monitored over several weeks.

Cu 2p peak; see the Supporting Information for data). In high-resolution scans, we observed the characteristic pattern for copper(I), which consists of two peaks owing to spin–orbit coupling at 932 and 952 eV.

To investigate the sensing mechanism, we prepared field-effect transistor (FET) devices with **1**-SWNT and pristine SWNT. A device architecture with interdigitated Au electrodes (10 μm gap) on Si with 300 nm SiO_2 was used. We kept the source-drain potential at a constant bias of 0.1 V, while the source-gate potential was scanned between +2 and −20 V. We observed a slight linear increase in conductance towards negative gate voltages (see the Supporting Information for data); however, no strong gate effect. This lack of a measurable shift in the turn-on voltage may be the result of the fact that the charge injection (doping) differences are very small and/or due to device geometry and the nature of the nanotube network. In those cases where strong turn-on SWNT FET responses are observed at negative gate voltages, more highly ordered nanotube networks are usually employed.[12]

We then used our sensory system to compare the ethylene emission from a selection of common fruits (banana, avocado, apple, pear, and orange). In the experimental setup, the fruit was enclosed in the gas flow chamber as shown in Scheme 2, which allowed us to expose the devices to fruit volatiles in the same way as to ethylene. The responses of **1**-SWNT devices to the different fruits are shown in Figure 4 (top). The intensities are given in relation to the response to 20 ppm ethylene and normalized to 100 g fruit. We found the largest response for banana, followed by avocado, apple, pear, and orange. All fruit apart from orange showed ethylene concentrations above 20 ppm, which corresponds to emission rates exceeding 9600 nL min^{-1}. To follow the ripening and senescing process in these fruits, we repeatedly measured their ethylene emission over several weeks (Figure 4 (bottom)). Fruit can be classified into climacteric and non-climacteric fruit according to respiration rate (release of CO_2) and C_2H_4 production pattern.[1] Banana, avocado, apple, and pear belong to the climacteric group, which is characterized by a large increase in CO_2 and C_2H_4 production during ripening, while non-climacteric fruits, such as orange, generally show low emission rates of these gases. Once the climax (ripeness) is achieved, respiration and C_2H_4 emission decrease as the fruit senesces. We were able to observe the climacteric rise during ripening in case of the pear and avocado, which showed an increased ethylene emission after the first week. For all other fruits and after the second week for the pear, measurements were conducted close to the maximum point of ripeness, and as a result our data reflects the senescence of the fruit with decreasing ethylene production rates for banana and apple. We compared two apples of the same kind and of similar ripeness, of which one was stored in a refrigerator (apple 1), while apple 2 was kept at room temperature. As anticipated, apple 2 senesced faster at room temperature, and hence its ethylene production decreased at a quicker pace than for apple 1. The orange as a non-climacteric fruit showed an overall low emission rate of ethylene.

To assess the selectivity of our sensory system, we measured the responses of **1**-SWNT devices to several solvents (75–200 ppm concentrations) as representatives of functional groups as well as to ethanol and acetaldehyde, which occur as fruit metabolites. The results are shown in Figure 5 in comparison to the response to 50 ppm ethylene and to pristine SWNTs.

We observed significantly high responses towards acetonitrile, THF, and acetaldehyde, while all other solvents had only small effects. However, considering the concentrations of these compounds, the responses are smaller in magnitude than the response to ethylene (50 ppm ethylene vs. 100 ppm acetonitrile, 200 ppm THF or 75 ppm acetaldehyde). The sensitivity of **1**-SWNT devices towards these analytes is not

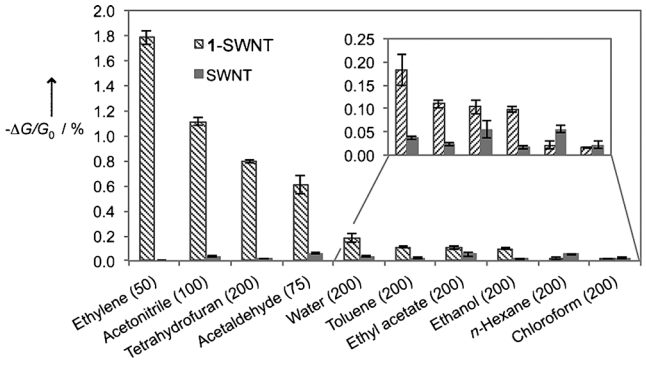

Figure 5. Relative responses of **1**-SWNT devices and pristine SWNT to 50 ppm ethylene and various solvents diluted with nitrogen gas (respective concentrations are given in parentheses in ppm).

surprising, as they are able to bind to the copper center in **1** by, for example, the nitrile group in acetonitrile or the oxygen of acetaldehyde with binding strengths comparable to that of ethylene (see the Supporting Information).

The concentrations required for fruit ripening lie in most cases between 0.1 and 1 ppm, and hence in storage facilities the ethylene level is to be kept below those thresholds. Our sensory system consisting of **1** and SWNTs shows good responses down to 1 ppm of ethylene. We found that we can further improve the sensitivity by increasing the surface area and porosity of the SWNT network structure. To achieve this, we added 5 wt % cross-linked polystyrene beads of 0.4–0.6 μm diameter to the mixture from which devices were prepared. Scanning electron microscope (SEM) images of the devices confirm a higher surface roughness for **1**-PS-SWNT devices compared to **1**-SWNT devices and the presence of SWNT bundles on the polymer beads for **1**-PS-SWNT (see the Supporting Information). The responses of the resulting **1**-PS-SWNT devices to ethylene concentrations of 0.5, 1, and 2 ppm are shown in Figure 6. A 1.3–2.2-fold increase in sensitivity was observed, which we attribute to an increased surface area of the SWNT network and possibly an increase in the local ethylene concentration in the device by partitioning into the polystyrene beads.

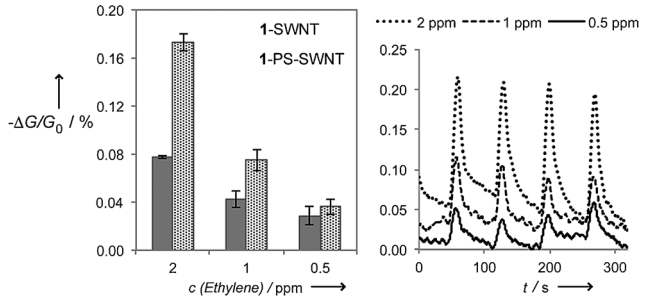

Figure 6. Comparison of the responses of **1**-SWNT devices and **1**-PS-SWNT devices to 0.5, 1, and 2 ppm ethylene.[8]

In summary, we have developed a carbon nanotube based sensor for ethylene gas in which copper(I) complexes are employed for the specific recognition of ethylene. The sensory material is simple to prepare and allowed us to detect sub-ppm concentrations of ethylene. We further demonstrated that sensitivity can be enhanced by adding polystyrene particles. The sensory system shows good selectivity and allowed us to follow the ripening and senescing processes in different fruit.

Experimental Section

Preparation of **1**: $(CF_3SO_3Cu)_2{\cdot}C_6H_6$ (8 mg, 15.9 μmol) was dissolved in dry, degassed toluene (3 mL). Hydrotris[3,5-bis(trifluoromethyl)-pyrazol-l-yl]borato sodium ($Na[HB(3,5\text{-}(CF_3)_2\text{-}pz)_3]$; 17 mg, 43.5 μmol)[13] was added, and the mixture was stirred for 14 h at RT. The reaction mixture was filtered to give a colorless solution of **1** with a concentration of about 6 μmol mL^{-1} (6 mM; the exact concentration was determined by NMR spectroscopy).

Preparation of **1**-SWNT: SWNTs (SWeNT SG65; 0.50 mg, 41.6 μmol carbon) were suspended in dry *o*-dichlorobenzene (0.8 mL), and a 6 mM solution of **1** in toluene (1.16 mL, 6.9 μmol) was added. The mixture was sonicated at 30 °C for 30 min. The resulting black dispersion of **1**-SWNT was used to prepare devices.

In the case of **1**-PS-SWNT a suspension of cross-linked polystyrene particles in toluene (2.4 μL,5 μg mL^{-1}) was added before sonication.

Received: February 7, 2012
Published online: April 19, 2012

Keywords: copper · ethylene · hormones · nanotubes · sensors

[1] A. A. Kader, M. S. Reid, J. F. Thompson in *Postharvest Technology of Horticultural Crops* (Ed.: A. A. Kader), University of California, Agricultural and Natural Resources, Publication 3311, **2002**, pp. 39 ff.

[2] a) A. Theologis, *Cell* **1992**, *70*, 181–184; b) H. Kende, *Annu. Rev. Plant Physiol. Plant Mol. Biol.* **1993**, *44*, 283–307.

[3] a) D. R. Kauffman, A. Star, *Angew. Chem.* **2008**, *120*, 6652–6673; *Angew. Chem. Int. Ed.* **2008**, *47*, 6550–6570; b) J. M. Schnorr, T. M. Swager, *Chem. Mater.* **2011**, *23*, 646–657.

[4] a) F. I. Rodríguez, J. J. Esch, A. E. Hall, B. M. Binder, G. E. Schaller, A. B. Bleecker, *Science* **1999**, *283*, 996–998; b) B. M. Binder, *Plant Sci.* **2008**, *175*, 8–17.

[5] a) H. Pham-Tuan, J. Vercammen, C. Devos, P. Sandra, *J. Chromatogr. A* **2000**, *868*, 249–259; b) M. Scotoni, A. Rossi, D. Bassi, R. Buffa, S. Iannotta, A. Boschetti, *Appl. Phys. B* **2006**, *82*, 495–500; c) L. R. Jordan, P. C. Hauser, G. A. Dawson, *Analyst* **1997**, *122*, 811–814; d) M. A. G. Zevenbergen, D. Wouters, V.-A. T. Dam, S. H. Brongersma, M. Crego-Calama, *Anal. Chem.* **2011**, *83*, 6300–6307; e) O. Green, N. A. Smith, A. B. Ellis, J. N. Burstyn, *J. Am. Chem. Soc.* **2004**, *126*, 5952–5953.

[6] B. Esser, T. M. Swager, *Angew. Chem.* **2010**, *122*, 9056–9059; *Angew. Chem. Int. Ed.* **2010**, *49*, 8872–8875.

[7] a) H. V. R. Dias, H.-L. Lu, H.-J. Kim, S. A. Polach, T. K. H. H. Goh, R. G. Browing, C. J. Lovely, *Organometallics* **2002**, *21*, 1466–1473; b) for a review on coinage-metal–ethylene complexes, see: H. V. R. Dias, J. Wu, *Eur. J. Inorg. Chem.* **2008**, 509–522.

[8] The data plotted is the floating average over 5 s of the original data.

[9] Calculations were performed using Gaussian 03 (Gaussian 03, Revision E.01, M. J. Frisch et al., Gaussian, Inc., Wallingford CT, **2004**; see Supporting Information for complete citation), the

B3LYP functional and as basis sets 6-31G* for C, H, B, F, N and LanL2DZ for Cu. Minima were characterized by harmonic vibrational frequency calculations. Energetic and structural data for all optimized compounds can be found in the Supporting Information.

[10] Owing to limitations of computational power, a harmonic vibrational frequency calculation could not be performed on **3**. The energy given was calculated using electronic energies.

[11] A. Jorio, M. Dresselhaus, R. Saito, G. F. Dresselhaus, in *Raman Spectroscopy in Graphene Related Systems*, Wiley-VCH, Weinheim, **2011**, pp. 327 ff.

[12] a) B. L. Allen, P. D. Kichambare, A. Star, *Adv. Mater.* **2007**, *19*, 1439 – 1451; b) R. Martel, T. Schmidt, H. R. Shea, T. Hertel, Ph. Avouris, *Appl. Phys. Lett.* **1998**, *73*, 2447 – 2449; c) S. Auvray, V. Derycke, M. Goffman, A. Filoramo, O. Jost, J.-P. Bourgoin, *Nano Lett.* **2005**, *5*, 451 – 455.

[13] H. V. R. Dias, W. Jin, H.-J. Kim, H.-L. Lu, *Inorg. Chem.* **1996**, *35*, 2317 – 2328.

